Cocrystallization and Phase Segregation of Polyethylene Blends between the D and H Species. 6. Time-Resolved FTIR Measurements for Studying the Crystallization Kinetics of the Blends under Isothermal Conditions

Kohji Tashiro,*,† Masaaki Izuchi,† Fumiko Kaneuchi,‡ Chihiro Jin,‡ Masamichi Kobayashi,† and Richard S. Stein§

Department of Macromolecular Science, Faculty of Science, Osaka University, Toyonaka, Osaka 560, Japan, Japan Spectroscopic Company Ltd., Ishikawa-Cho, Hachioji, Tokyo 192, Japan, and Polymer Research Institute, University of Massachusetts, Amherst, Massachusetts 01003

Received August 10, 1993; Revised Manuscript Received November 24, 1993®

ABSTRACT: In order to clarify the origin of the cocrystallization and phase segregation phenomena observed for a series of polyethylene blends between the deuterated and hydrogeneous species, time-resolved Fourier-transform infrared spectroscopic measurements have been performed under isothermal crystallization conditions by controlling the degree of undercooling or the temperature jump depth from the molten state to the isothermal crystallization temperature. A closeness of the crystallization rate between the pure D and H species was found to correlate well with the occurrence of the cocrystallization phenomenon. In the cocrystallizable blend sample, the crystallization rates of the D and H components were found to be almost the same and accelerated remarkably when compared with those of the individual pure components. The mechanism of cocrystallization and phase segregation was discussed from the viewpoints of both thermodynamics and kinetics.

Introduction

In a series of papers,[1-5] we have investigated the phenomena of cocrystallization and phase segregation occurring in polyethylene (PE) blends between deuterated high-density PE (DHDPE) and hydrogeneous PE with various degrees of ethyl side-chain branching. The tendency of cocrystallization and phase segregation is dependent on the degree of branching and the blend content of the D and H species. For example, the linear low-density PE [LLDPE(2)] with ca. 17 branching/1000 carbons can cocrystallize almost perfectly with DHDPE for any D/H content even when the sample is slowly cooled from the melt. On the other hand, the DHDPE blend with LLDPE(3) of ca. 41 branching or HDPE without branching shows preferably the phase segregation phenomenon: the CD_2 and CH_2 crystalline lamellae exist separately from each other. But this tendency is affected to some extent by the D/H blend content, and some degree of cocrystallization is induced when the H (or D) species is diluted in the blend: that is, some of the isolated H chains are trapped to cocrystallize with the surrounding D chains.

A clarification of the origin of these phenomena may provide us very important information to understand the essence of crystallization behavior of PE and also the key factors governing the miscibility of the blend samples. It was pointed out that factors such as the closeness between the D and H species in molecular weight, molecular weight distribution, crystallization temperature, unit cell parameters, etc., do not have a very strong correlation with these crystallization phenomena as far as the present blend samples are concerned. Another important factor which has not yet been considered may be the closeness in crystallization rate of the D and H species or the mobility of these chains.

In order to clarify this problem, we have tried to measure the crystallization rate for these blend systems. In this case, it is very important to compare the rates of the D (or H) species among the different samples and also the rates of the D and H species in the blend. That is to say, we need to measure the crystallization behavior of both the D and the H species simultaneously and with enough high-resolution power. Fourier-transform infrared spectroscopic (FTIR) measurement is considered to be best for this purpose, because the spectrum in the whole frequency region can be obtained in a single scan of the Michelson interferometer in a very short time of milliseconds to seconds. At the same time, in order to trace the higher order structural change in the sample, we need to measure the X-ray diffraction as a function of time.[6-9] Another method for this purpose may be the measurement of wide-angle neutron scattering (WANS) and small-angle neutron scattering (SANS) as a function of time based on their potentiality of differentiating the D and H species. But it is technically quite difficult to carry out such a time-resolved neutron measurement at present.

In this paper, we will report the experimental results concerning the time-resolved FTIR measurements for a series of PE blend samples. The thus obtained data are combined together with the already reported thermodynamic data, and the crystallization mechanism will be discussed from the microscopic point of view.

Experimental Section

Samples. DHDPE was purchased from Merck Chemical Co., Ltd. The hydrogeneous polyethylene samples with different degrees of branching, i.e., high-density polyethylene (HDPE) and two types of linear low-density polyethylene [LLDPE(2) and LLDPE(3)], were supplied from Exxon Chemicals Co., Ltd.

† Osaka University.
‡ Japan Spectroscopic Co. Inc.
§ University of Massachusetts.
® Abstract published in *Advance ACS Abstracts*, February 1, 1994.

0024-9297/94/2227-1240$04.50/0

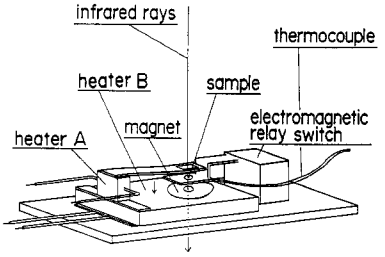

Figure 1. Schematic diagram of the temperature jump apparatus for FTIR measurement.

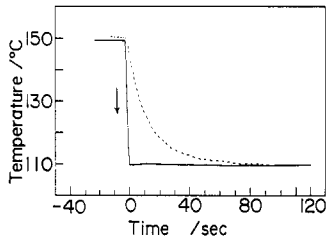

Figure 2. Example of the temperature jump from 150 to 110 °C attained by the apparatus shown in Figure 1: (—) air flow blown up to the sample holder; (- - -) no air flow.

Table 1. Characterization of PE Samples

	M_w	M_n	M_w/M_n	branching/1000 C
DHDPE	80K	14K	5.7	2-3
HDPE	126K	24K	5.3	1
LLDPE(2)	75K	37K	2.0	17
LLDPE(3)	61K	20K	3.1	41

For the LLDPE samples, the side chain is the ethyl group. The characterization of these samples is listed in Table 1. The blends were prepared by dissolving the D and H species of 25:75, 50:50, or 75:25 wt % ratio into boiling *p*-xylene with a concentration of about 2 wt % and by precipitating it into methanol at room temperature. Samples were melted and pressed on a hot plate at ca. 150 °C and then cooled slowly to room temperature. The film thickness was ca. 30 μm for infrared measurements.

Temperature Jump Method. In the crystallization kinetics experiment, the most important technique to be developed is how fast the temperature of the sample can be changed from the molten state to the predetermined point. In the case of PE, the crystallization occurs on the order of milliseconds to seconds to minutes depending on the degree of undercooling.[10] Therefore, we consumed our energy in preparing the temperature jump apparatus as described here.

In Figure 1 is illustrated an optical cell used for the time-resolved FTIR measurement. A sample film was fixed securely on the stainless steel holder and set on the end of the arm of the electromagnetic relay. The sample was melted by being contacted with heater A, the temperature of which was kept constant at ca. 160 °C (the temperature was monitored by a Chromel-Alumel thermocouple). This molten sample was moved down as quickly as possible by utilizing an electromagnetic relay switch: the metal plate arm was moved between the S and N poles of the electromagnet by switching the circuit on and off. A permanent magnet on heater B helped to accelerate the movement of the metal holder, to stabilize the sample position, and to increase good contact between the sample and magnet surface. This permanent magnet was kept at a predetermined temperature where the crystallization occurred. The speed of temperature drop was not high when the sample was moved simply between these two heaters. Then a flow of air was blown up to the sample so as to get the heat on the sample away and then to increase the cooling rate. The attained temperature jump is reproduced in Figure 2, where the cooling rate could be increased up to about 600 °C/min.

The thus constructed optical cell was set into the microscope FTIR installment. This microscope was useful because the sample size needed to be as small as possible in order to minimize the heat flow within the sample and also because the sample was installed horizontally so as to escape from flowing down and

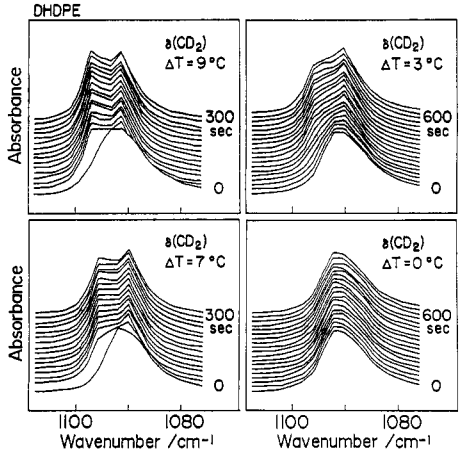

Figure 3. Time dependence of the infrared spectra measured for the pure DHDPE sample at ΔT = 9, 7, 3, and 0 °C.

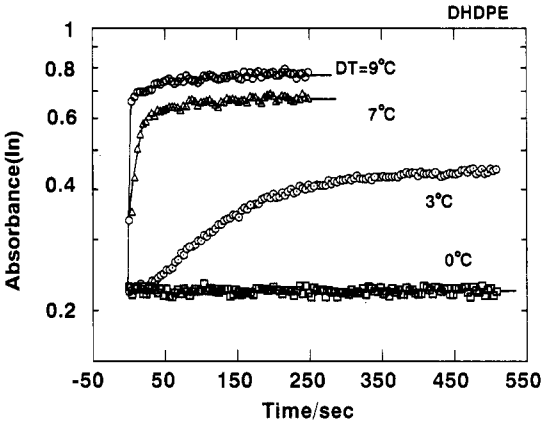

Figure 4. Time dependence of the crystalline $\delta(CD_2)$ band intensity of the pure DHDPE sample measured at various undercoolings.

to make it easier to carry out the experiment. The used FTIR microscope was a Japan Spectroscopic Co. "Janssen" FTIR microscope with a special software program prepared for time-resolved measurements. The time interval of measuring, transforming, and saving one spectrum was about 4 s for the resolution power of 4 cm^{-1} and the accumulation time of one.

Results and Discussion

Comparison of Crystallization Rates among Pure Samples. The crystallization rate is influenced sensitively by the degree of undercooling (ΔT), which is defined as a difference between the crystallization temperature (T°_c) and the predetermined temperature (T_c): $\Delta T = T^\circ_c - T_c$. For T°_c, a value was employed which was estimated from the static measurement of the temperature dependence of the infrared spectra reported in our previous papers. ΔT in this experiment was 9, 6, 3, and 0 °C. For example, Figure 3 shows the time-resolved infrared spectral changes of the CD_2 bending [$\delta(CD_2)$] band measured for the pure DHDPE sample at various ΔT's. In Figures 4–7 are plotted the time dependencies of the peak intensities of $\delta(CH_2)$ or $\delta(CD_2)$ measured for samples DHDPE, HDPE, LLDPE-(2), and LLDPE(3), respectively, where the peak intensities at 1468 cm^{-1} (CH_2) and 1092 cm^{-1} (CD_2) were evaluated. (Of course, the integrated intensity may be better than the peak intensity in such a discussion, but the number of data are too much to carry out the integration for all the spectra measured as functions of time.) The rate of growth of the crystalline band intensity is very sensitive to ΔT. In addition, the finally achieved absorbance decreases with the smaller ΔT, relating reasonably with the crystallinity attained at T_c. The slope of the curve is

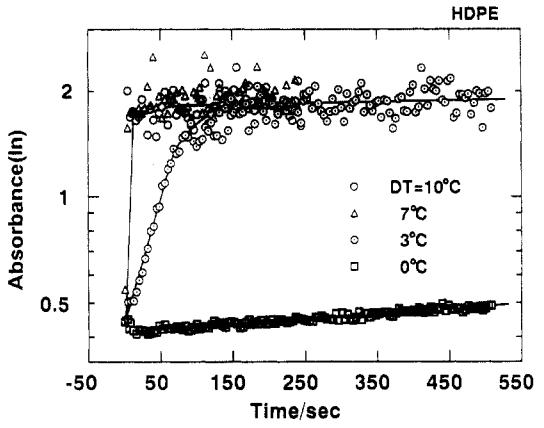

Figure 5. Time dependence of the crystalline $\delta(CH_2)$ band intensity of the pure HDPE sample measured at various undercoolings.

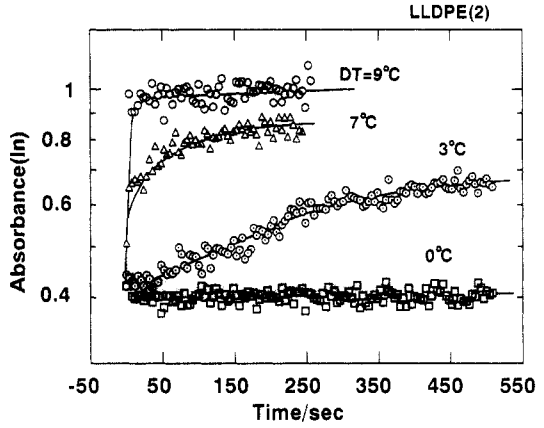

Figure 6. Time dependence of the crystalline $\delta(CH_2)$ band intensity of the pure LLDPE(2) sample measured at various undercoolings.

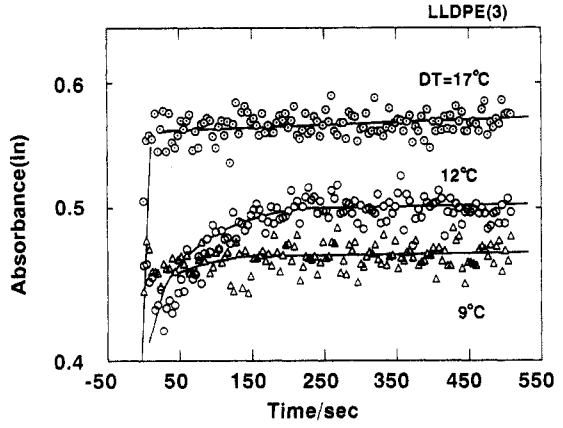

Figure 7. Time dependence of the crystalline $\delta(CH_2)$ band intensity of the pure LLDPE(3) sample measured at various undercoolings.

a measure of the crystallization rate. For a common ΔT, the slope differs largely among the samples with different branching content. In Figure 8 are compared the time dependencies of infrared absorbance measured for the pure PE samples at ΔT = 3 °C. As the degree of branching increases from HDPE to LLDPE(2) and to LLDPE(3), the crystallization rate decreases drastically. From Figure 8, it is clearly said that the order of crystallization rate is as follows for the pure samples: HDPE > DHDPE ≈ LLDPE(2) ≫ LLDPE(3). That is to say, DHDPE crystallizes at a rate very similar to that of LLDPE(2). The crystallization rate of HDPE is appreciably high and that of LLDPE(3) is too low compared with that of DHDPE.

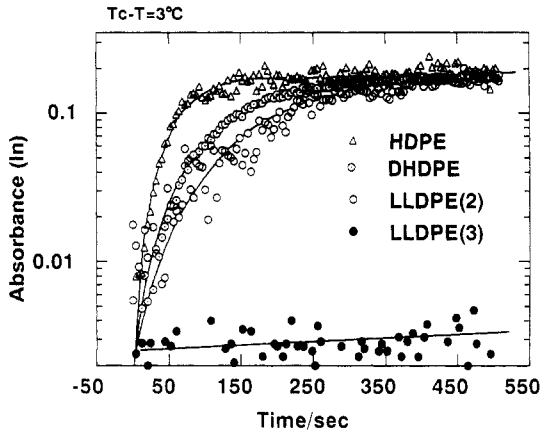

Figure 8. Comparison in the time dependence of the crystalline band intensity between the pure PE samples measured at ΔT = 3 °C.

In a previous paper, we clarified that DHDPE and LLDPE(2) are most compatible thermodynamically as judged from the data of DSC and static measurement of the temperature dependence of the infrared spectra. Figure 8 indicates that these two samples are also compatible in the point of crystallization kinetics. Let's assume that the D and H chains can dissolve each other in the molten state (this assumption is now being checked experimentally by the measurement of small-angle neutron scattering). On crystallization from the melt, the chains diffuse to gather together so as to form the crystalline nuclei. Once such a crystalline nucleus is formed, then the crystalline domain begins to grow with time. That is to say, the crystallization rate is determined by both the diffusion rate of the chains and the growth rate of the nuclei. The above experimental data suggest that the DHDPE and LLDPE(2) chains will escape from the molten state to cocrystallize together at almost the same rate. Besides, they are thermodynamically compatible; i.e., the coexistence within the same crystallite is thermodynamically more advantageous than the occurrence of phase segregation. In the case of DHDPE/LLDPE(3) and DHDPE/HDPE, one component (the D species for the former and the H species for the latter) crystallizes too fast compared with the other component, resulting in phase separation. (Of course, it should not be ignored that some portion of the slow component is induced to cocrystallize with the other component of higher crystallization rate.) These speculations may be checked by measuring the crystallization rates of both the H and D components in the blends as described below.

Crystallization Rates of the H and D Components in the Blends. For example, Figure 9 shows the results for DHDPE/LLDPE(2) samples. For all samples of different D/H content, the CH_2 and CD_2 crystalline bands are found to increase their intensities at almost the same rate, supporting the above-mentioned crystallization model. It should be noticed here that the crystallization rate is appreciably enhanced in the blend compared with the case of the pure samples, as shown in Figure 10. This acceleration effect might originate from the thermodynamic compatibility between the D and H chains. That is to say, both species are energetically more advantageous when mixed up together, and such a thermodynamic advantage will act as a driving force to enhance the growing rate of the cocrystals.

Figure 11 shows the result for the DHDPE/LLDPE(3) 50/50 wt % blend sample. For ΔT = 3 °C, only the D chains crystallize and most of the H chains remain melted. "Most" means that some of the H component cocrystallizes

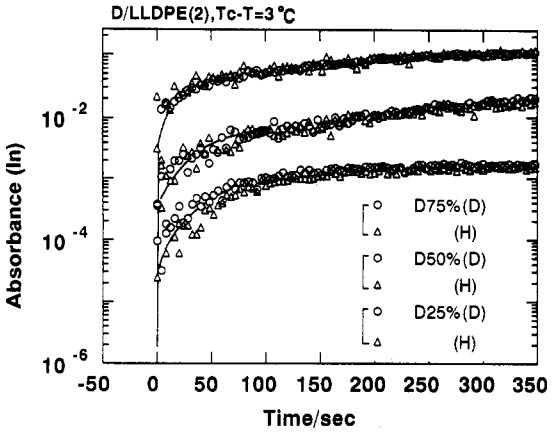

Figure 9. Comparison of the crystallization rate between the H and D components in DHDPE/LLDPE(2) blends with various D/H contents.

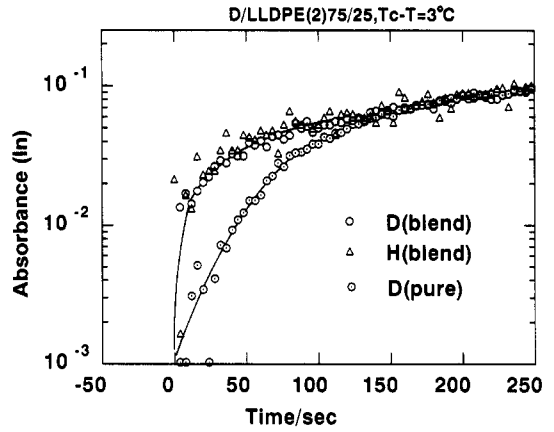

Figure 10. Time dependencies of the infrared crystalline band intensity measured for the D and H components in the DHDPE/LLDPE(2) 75/25 wt % blend and for the pure DHDPE sample.

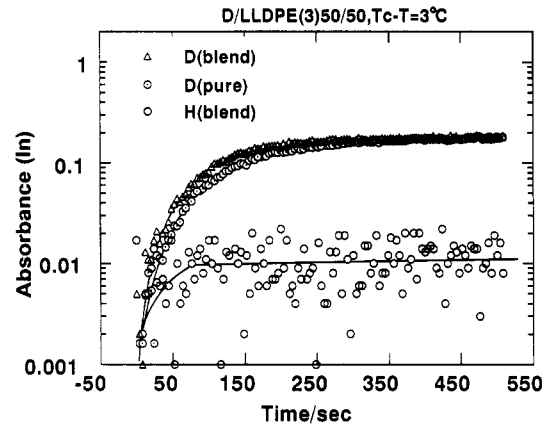

Figure 11. Time dependencies of the infrared crystalline band intensity measured for the D and H components in the DHDPE/LLDPE(3) 50/50 wt % blend and for the pure DHDPE sample.

with the D species. This can be observed more clearly in the case of the DHDPE/LLDPE(3) 75/25 wt % sample shown in Figure 12. In this case, some portion of the H chains are detected to crystallize together at almost the same rate with that of D chains, although most of the H chains are still melted. This is just coincident with the discussion made before: in an early stage of crystallization of the D chains, the H chains are induced to cocrystallize together. The kinetic study also confirms it clearly.

Figure 13 shows the result for the DHDPE/HDPE 50/50 wt % blend sample. For ΔT = 3 °C, the H chains crystallize at a high rate but the D chains are almost not detected to crystallize. Strictly speaking, however, some

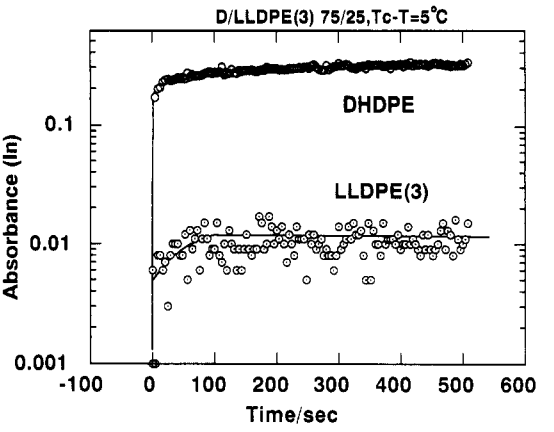

Figure 12. Time dependencies of the infrared crystalline band intensity measured for the D and H components in the DHDPE/LLDPE(3) 75/25 wt % blend.

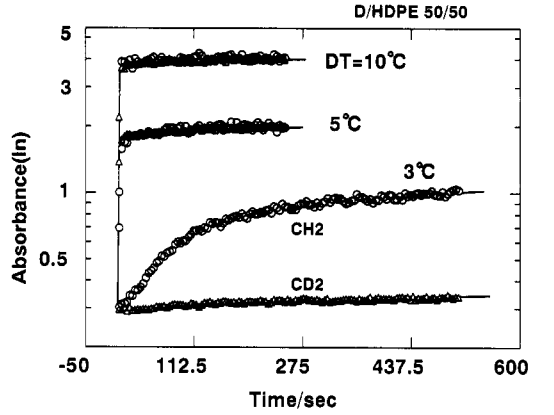

Figure 13. Comparison of the crystallization rate between the H and D components in the DHDPE/HDPE 50/50 wt % blend at various undercoolings.

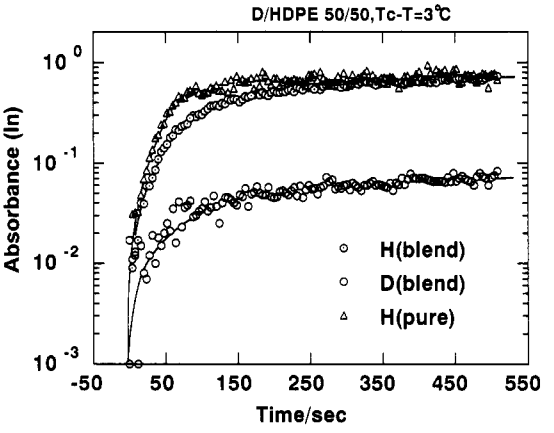

Figure 14. Time dependencies of the infrared crystalline band intensity measured for the D and H components in the DHDPE/HDPE 50/50 wt % blend and for the pure DHDPE sample.

of the D chains are found to crystallize at almost the same rate with that of the H component, as seen in Figure 14. In contrast to the acceleration effect seen in the cases of the blend systems of DHDPE/LLDPE(2) and DHDPE/LLDPE(3), the crystallization rate of the H chains decreases slightly compared with the rate of the pure HDPE sample. An existence of D chains, which cocrystallizes simultaneously during the crystallization of the H chains, may reduce the diffusion rate of the H chains, resulting in a reduction of crystallization rate of the H chains.

In this way, the study of crystallization kinetics gives us useful information on the crystallization mechanism of this blend system. As discussed above, whether the

cocrystallization occurs or not is determined by a balance between the thermodynamic and kinetic factors between the CD_2 and CH_2 components. Even when the D and H chains crystallize at almost the same rate, they cannot cocrystallize at all if their coexistence is thermodynamically disadvantageous. On the contrary, if the crystallization rate is different between the D and H species, then they are difficult to cocrystallize even if they are thermodynamically intimate with each other.

In the FTIR measurement described in this paper, the resolutions of time and wavenumber are not very high but only about 4 s and 4 cm^{-1}, respectively. They are too low to discuss the details of interactions between chains in an early stage of crystallization. Now we are trying to measure the time-resolved FTIR of the PE blends with more sophisticated installment having a higher resolution power of time and wavenumber. Concerning the phenomena of cocrystallization and phase segregation in PE blends, the next problem to be solved may be a clarification of the reasons why and how the branching and the blend content decide the compatibility between the D and H species. Molecular theoretical development may be required to solve these problems.

References and Notes

(1) Tashiro, K.; Stein, R. S.; Hsu, S. L. *Macromolecules* **1992**, *25*, 1801.
(2) Tashiro, K.; Satkowski, M. M.; Stein, R. S.; Li, Y.; Chu, B.; Hsu, S. L. *Macromolecules* **1992**, *25*, 1809.
(3) Tashiro, K.; Izuchi, M.; Kobayashi, M.; Stein, R. S. *Macromolecules*, preceding paper in this issue.
(4) Tashiro, K.; Izuchi, M.; Kobayashi, M.; Stein, R. S. *Macromolecules*, preceding paper in this issue.
(5) Tashiro, K.; Izuchi, M.; Kobayashi, M.; Stein, R. S. *Macromolecules*, preceding paper in this issue.
(6) Schultz, J. M. *J. Polym. Sci., Polym. Phys. Ed.* **1976**, *14*, 2291.
(7) Schultz, J. M.; Lin, J. S.; Hendricks, R. W. *J. Appl. Crystallogr.* **1978**, *11*, 551.
(8) Song, H. H.; Stein, R. S.; Wu, D. Q.; Ree, M.; Philips, J. C.; LeGrand, A.; Chu, B. *Macromolecules* **1988**, *21*, 1180.
(9) Song, H. H.; Wu, D. W.; Chu, B.; Satkowski, M.; Stein, R. S.; Philips, J. C. *Macromolecules* **1990**, *23*, 1280.
(10) Pakula, T.; Kryszewski, M. *Polym. J.* **1976**, *12*, 47.